Decellularization techniques of human foreskin for tissue engineering application

Olga NOVOTNA[1], Zuzana VARCHULOVA NOVAKOVA[2], Paulina GALFIOVA[3], Maria LORENCOVA[3], Martin KLEIN[3], Stanislav ŽIARAN[4], Marcela KUNIAKOVA[2],

[1]Department of Pediatric Urology, National Institute of Children's Diseases, Faculty of Medicine, Comenius University in Bratislava, Bratislava, Slovakia, [2]Institute of Medical Biology, Genetics and Clinical Genetics, Faculty of Medicine, Comenius University in Bratislava, Bratislava, Slovakia, [3]Institute of Histology and Embryology, Faculty of Medicine, Comenius University in Bratislava, Bratislava, Slovakia, [4]Department of Urology, Faculty of Medicine, Comenius University, Bratislava, Slovakia

Received June 30, 2023
Accepted July 7, 2023

Summary

The rapid development of tissue engineering (TE) and regenerative medicine brings an acute need for biocompatible and bioactive biological scaffolds to regenerate or restore damaged tissue. Great attention is focused on the decellularization of tissues or even whole organs, and the subsequent colonization of such decellularized extracellular matrices by recipient cells. The foreskin is an integral, normal part of the external genitalia that forms the anatomical covering of the glans penis and the urinary meatus of all human and non-human primates. It is mucocutaneous tissue that marks the boundary between mucosa and skin. In this work, we compared two innovative decellularization techniques for human foreskins obtained from donors. We compared the efficacy and feasibility of these protocols and the biosafety of prepared acellular dermal matrixes that can serve as a suitable scaffold for TE. The present study confirms the feasibility of foreskin decellularization based on enzymatic or detergent methods. Both techniques conserved the ultrastructure and composition of natural ECM while being DNA-free and non-toxic, making it an excellent scaffold for follow-up research and TE applications.

Keywords

Foreskin • Decellularization • Scaffold • Tissue engineering

Corresponding author

M. Kuniakova, Institute of Medical Biology, Genetics and Clinical Genetics, Faculty of Medicine, Comenius University in Bratislava, Sasinkova 4, 811 08 Bratislava, Slovakia, Email: marcela.kuniakova@fmed.uniba.sk

Introduction

The rapid development of tissue engineering (TE) and regenerative medicine brings an acute need for biocompatible and bioactive biological scaffolds to regenerate or restore damaged tissue. Great attention is focused on the decellularization of tissues or even whole organs, and the subsequent colonization of such decellularized extracellular matrices by recipient cells.

Acellular dermal matrix (ADM) is an allograft tissue that has undergone processing to preserve the extracellular matrix while removing all cellular components [1]. It functions by supplying a bioactive substance made up of collagen fibers and bundles, proteins, intact elastin, hyaluronic acid, fibronectin, fibrillar collagen, type VI collagen, vascular channels, proteoglycans, and bioactive proteins that support tissue remodeling, revascularization, and cell repopulation [2]. ADM is widely used in many medical applications, for example in reconstructive and aesthetic surgery [3,4], stomatology [5,6], the therapy of full-thickness skin defects [7,8], and genitourinary reconstructive surgery [9-11]. Researchers are forced to hunt for alternatives due to the rising demand for skin grafts and substitutes, as well as the global donor shortage. Decellularization is used to create allogenic ADM from human cadaveric donor skin dermal tissue and xenogeneic ADM from animal skin donor sources. The utilization of

an autologous tissue source is frequently linked to morbidity at the donor site. Although scientific organizations have already created several procedures for tissue decellularization, typically by combining physical, chemical, and enzymatic techniques, there is currently no methodological gold standard for the process [12]. The specification of the tissue, including its size and origin, as well as the intended application of the processed sample, will determine the most appropriate procedure to apply.

The foreskin, also known as the prepuce is an integral, normal part of the external genitalia that forms the anatomical covering of the glans penis and the urinary meatus of all human and non-human primates. The prepuce is a specialized, mucocutaneous tissue that marks the boundary between mucosa and skin. It is a double-layered fold of skin, mucosal and muscular tissue at the most distal end of the human penis. The foreskin is attached to the glans by an elastic band of tissue, known as the frenulum. The outer skin of the foreskin meets with the inner preputial mucosa at the area of the mucocutaneous junction [13]. The foreskin is mobile, relatively stretchable, has a protective function of decreasing external irritation or contamination, and sustains the glans in a moist environment. Foreskin length varies widely, according to Werker *et al.* the mean surface area of the prepuce, when folded out, is 46.7 cm^2 [14], Kigozi *et al.* reported in a larger cohort of patients the surface area, depending on age, is from 35.0 cm^2 to 38.4 cm^2 [15]. Removal of the foreskin by circumcision is most commonly performed as an elective procedure for prophylactic, cultural, or religious reasons [16]. Circumcision may be performed on children or adults to treat phimosis, dyspareunia, balanitis, and other pathologies with a low complication rate [17]. Male circumcision is also recommended by WHO/United Nations Joint Programme on HIV/AIDS (UNAIDS) as an HIV prevention strategy [18] because according to several studies, male circumcision reduces the risk of male HIV acquisition by 50–60 % [19,20]. Tissue obtained from circumcision procedures can be used as a source of fibroblasts for biomedical research [21] or as skin graft tissue [22].

In this work, we compared two innovative decellularization techniques for human foreskins obtained from donors. We compared the efficacy and feasibility of these protocols and the biosafety of prepared acellular dermal matrixes that can serve as a suitable scaffold for TE.

Material and Methods

Human donor foreskin harvesting

The human foreskin was harvested in accordance with the current regulations and with permission from the Institution for Healthcare Provider Surveillance Authority (EK/6/2/2022) in the Department of Pediatric Urology, National Institute of Children's Diseases. Male foreskins (n=12) were harvested under antiseptic conditions from boys aged three years to fifteen years for therapeutic purposes. After excision of outer and inner preputial skin layers, the samples were placed in a sterile collection solution comprised of 500 mg Edicin (Sandoz, Switzerland), 2 × 10^6 U Penicillin (Biotika, Slovakia), 200 mg Clotrimazole (Ratiopharm, Germany), 240 mg Gentamycin (Sandoz, Switzerland) per liter of saline), and transferred to the laboratory and left at 4 °C for 3 hours. The sample was then taken out of the solution and frozen at -20 °C without cryoprotectant.

Decellularization protocol

12 samples were divided into two groups (n = 6). To decellularize the foreskin, we looked at two approaches: enzyme (E) and detergent (D) protocol. The steps are summarized in Table 1.

E protocol - After thawing, the samples were moved to a new container containing 0.25 % trypsin-EDTA solution (Merck, Germany), and they are

Table 1. Summary of decellularization methods.

E protocol		D protocol	
Solution	**Temperature, Time**	**Solution**	**Temperature, Time**
Freeze-thaw	-20 °C	Freeze-thaw	-20 °C
0.25 % Trypsin-EDTA	4 °C, 24h	TRITON™ X-100 1:100 in dH_2O	4 °C, 24h
0.25 % Trypsin-EDTA	37 °C, 3h	dH_2O	4 °C, 2 x 10min
dH2O	20 °C, 2 x 10min	SDS 1 %	20 °C, 24h
DNase I 200µg/ml dH_2O	37 °C, 3h 4 °C, 72h	DNase I 200µg/ml dH_2O	37 °C, 3h 4 °C, 72h

incubated at 4 °C for 24 hours with constant mixing on an orbital shaker. Following 24 hours, the samples were incubated in the same solution at 37 °C for 3 hours. The epidermis was then mechanically separated from the dermis using tweezers on a sterile petri dish (Fig. 1). After epidermis removal, samples were washed twice with dH_2O. In the next step, samples were incubated for 3h at 37 °C in DNase I (200µg/ml; Roche, Switzerland). Specimens were then placed in a sterile container containing hypotonic solution-deionized water (dH_2O), incubated at 4 °C, and relocated daily into a new container with dH_2O for three consecutive days.

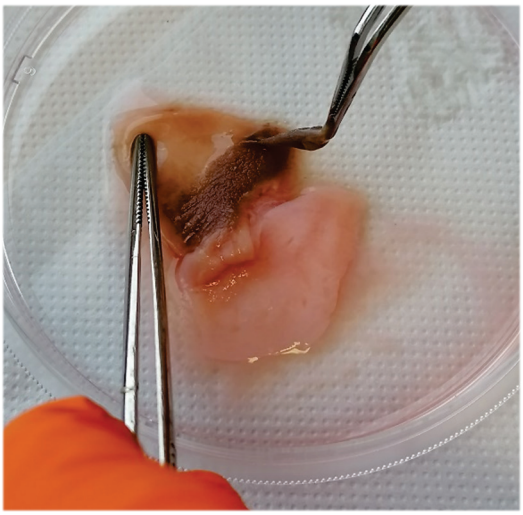

Fig. 1. Macroscale appearance of the human foreskin tissue - mechanical removal of the epidermis during the E protocol procedure.

D protocol - After thawing, the samples were transferred to a new container with TRITON™ X-100 (Merck, Germany) diluted 1:100 in dH_2O and washed for 24 h at 4 °C with agitation on an orbital shaker. After washing in dH_2O for 2 x 10 min, the samples were placed in a container with 1 % SDS solution (Merck, Germany) and washed for 24 h at 4 °C with agitation on an orbital shaker. After washing in dH_2O, samples were incubated for 3 h at 37 °C in DNase I (200 µg/ml; Roche, Switzerland). Then the samples were washed with dH_2O and relocated daily as mentioned above under gentle agitation for three days at 4 °C.

Light microscopy and immunohistochemistry (IHC)

We used the standard formalin-fixed, paraffin-embedded procedure to prepare the native controls and decellularized tissue samples of human male foreskin for light microscopy. The specimens were first fixed for 24 hours at room temperature in 10 % neutral buffered formalin (Centralchem, Slovakia), then dehydrated in a series of alcohol solutions with increasing alcohol concentrations up to 100 %, cleared with xylene (Merck, Germany) immersed in paraffin (Merck, Germany), and finally embedded in paraffin tissue blocks. The blocks were then cut into 5µm thick sections by a rotary microtome, transferred onto glass slides, deparaffinized using xylene, and rehydrated in alcohol series of decreasing concentrations to 50 %. To see cell nuclei, collagen fibers, and elastic fibers, the slides were next stained with hematoxylin and eosin (HE), blue trichrome, and orcein, respectively (all by Merck, Germany).

For IHC, antibodies against collagen IV and fibronectin (Merck, Germany) were used to visualize different components of the extracellular matrix (ECM). PT Link (Agilent Technologies, USA) was used to automatically carry out the pre-treatment procedures of deparaffinization, rehydration, and epitope unmasking. To stop endogenous peroxidase activity, the samples were exposed to a peroxidase-blocking reagent from the EnVision FLEX Detection system (Agilent Technologies, USA) for 5 minutes. The manufacturer's instructions were followed while applying the primary antibodies. Agilent Technologies (USA) EnVision FLEX Detection system's Diaminobenzidine (DAB)+ Chromogen was utilized for visualization. For better orientation within the native control specimens, cell nuclei were counterstained with Mayer's hematoxylin (Merck, Germany). The slides were examined by a LEICA DM2500 microscope, and representative fields of view were captured on the LEICA DFC290HD digital camera.

Scanning electron microscopy (SEM)

The native controls and decellularized tissue samples of human male foreskin were preserved in 3 % buffered glutaraldehyde (Merck, Germany) for 4 hours at room temperature in preparation for SEM. The maximum size of these samples was 600 mm3. The samples were then post-fixed in osmium tetroxide solution (Merck, Germany) at 4 °C and washed three times in sodium phosphate buffer (pH 7.3). The samples were then gently dehydrated with an alcohol series of increasing concentrations up to 100 % ethanol and dried at the critical point of CO_2 using a Critical Point Dryer, Leica EM CPD 300. The specimens were then mounted using carbon adhesive tapes on aluminum specimen stubs. The non-conductive specimens were sputter-coated with a 15 nm thick gold/palladium layer in the LEICA EM ACE200 sputter coater and observed by the ZEISS EVO LS 15 scanning electron microscope.

Analysis of DNA content

Using the GeneJET Genomic DNA Purification Kit (ThermoFisher Scientific, USA) methodology and agarose gel electrophoresis, DNA from control and decellularized samples was isolated, quantified, and analyzed. As a positive control, 12 naturally occurring foreskins, taken during a planned surgery from the same origin, were used. Briefly, foreskin samples were sliced into pieces and dried to a consistent weight at 37 °C. Following a precise weight measurement, a sample was reconstituted in Digestion Solution with Proteinase K (ThermoFisher Scientific, USA) and incubated at 56 °C for an extended period of time. RNase solution (ThermoFisher Scientific, USA) was added after incubation and let to sit for 10 minutes at room temperature. After that, a lysis solution was added, and the mixture was vortexed until it was homogenous. The lysate was transferred to a GeneJET Genomic DNA Purification Column (ThermoFisher Scientific, USA) and centrifuged after being vortexed with a 50 % ethanol solution (Centralchem, Slovakia). The Purification Column was moved to a sterile microcentrifuge tube after two rounds of washing, and an elution buffer was added to elute the genomic DNA. The final amount of DNA (ng/DNA per mg/tissue dry weight) was calculated after the concentration of the extracted DNA was determined spectrophotometrically using a Nanodrop Spectrophotometer (ThermoFisher Scientific, USA). 10 µl of total DNA were separated in a 1.5 % agarose gel for 40 minutes at 120 volts to perform a qualitative analysis of fragment length. The gel was photographed by the Azure C300 Imaging System (Azure Biosystems, USA) after the run.

Cytotoxicity assay – Growth inhibition assay

To verify whether the decellularized sample contains any soluble toxins we assessed the cytotoxicity of the matrix-conditioned medium on cells using the MTT Assay. Cell proliferation was used to evaluate the biocompatibility of the material, and 3-(4,5-dimethyl-2-thiazolyl)-2,5-diphenyl-2-H-tetrazolium bromide (MTT) was used to do so. First, 25 ml of DMEM (Merck, Germany) was added to 3 cm^2 of decellularized tissue, which was then shaken for 24 hours at 37 °C. After 24 hours, 10 % fetal bovine serum (FBS, Merck, Germany) was added after the medium had been filtered *via* a 0.2 µm filter. As a negative control, unconditioned DMEM supplemented with 10 % FBS was employed. A total of 7 x 10^3 adipose tissue-derived stem cells (ATSCs) were planted in replicates of six in a 96-well plate. The plates were incubated for 7 days at 37 °C in an environment humidified with 5 % CO_2. On days 1, 3, 5, and 7, one plate was taken out to perform the MTT assay, which measures cell viability. In each well containing 100 µl of culture media, 20 µl of CellTiter 96 AQueosus One Solution Cell Proliferation Assay (Promega, USA) was pipetted. The plate was incubated for 3 hours at 37 °C with 5 % CO_2 humidity. 96-well plate reader BioTek EL 800 (BioTek, USA) was used to measure absorbance at 490 nm. Data were collected, examined, and then transformed into graphs.

Statistical analysis

DNA content analysis results are reported as mean ± standard deviation (SD), with a statistical significance of $p < 0.001$. To compare and analyze the concentration of DNA isolated from dry tissue (ng/DNA per mg/tissue dry weight) from native foreskin samples with decellularized foreskin samples with respect to each other, a Student´s t-test was employed. Absorbance values are reported as mean ± SD.

Results

Decellularization of foreskin

Samples of human male foreskin were decellularized using either the enzyme Trypsin or the detergents Triton X-100 and SDS in two separate ways. After incubation in DNase and final washing steps, samples were subsequently characterized to verify decellularization success by histology, SEM, and analysis of remaining DNA. Testing for sterility and cytotoxicity verified the product's safety. The effectiveness of the decellularization process was first assessed by macroscopic appearance. Native foreskin samples after surgical removal *via* circumcision display a typical "butterfly" shape and pinkish appearance (Fig. 2A, 2B). In comparison to the inner foreskin, the epidermal layer in the outer regions has a different texture and seems slightly darker. After decellularization, the foreskin tissue displayed a color change to a milky white and slightly translucent state (Fig. 2C, 2D), indicating a vigorous cell elimination process. The E protocol showed a gentler color change (Fig. 2C), but histological analyses could not support lower levels of decellularization in those samples. Aerobic and anaerobic bacteria, fungi, and yeasts were not present in the cultures from either decellularization approach.

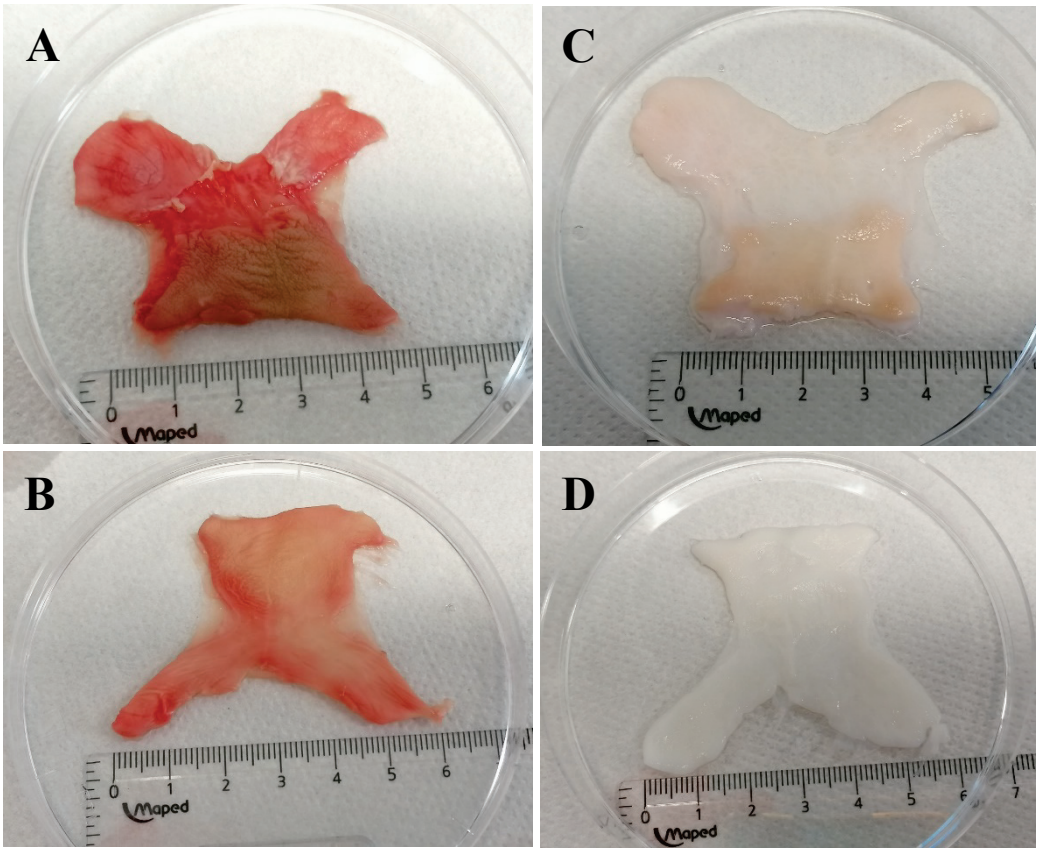

Fig. 2. Macroscale appearance of the human foreskin tissue: **A), B)** fresh frozen foreskin tissue prior to the decellularization process, **C)** foreskin dermal matrix, post-E protocol decellularization, **D)** foreskin dermal matrix, post-D protocol decellularization

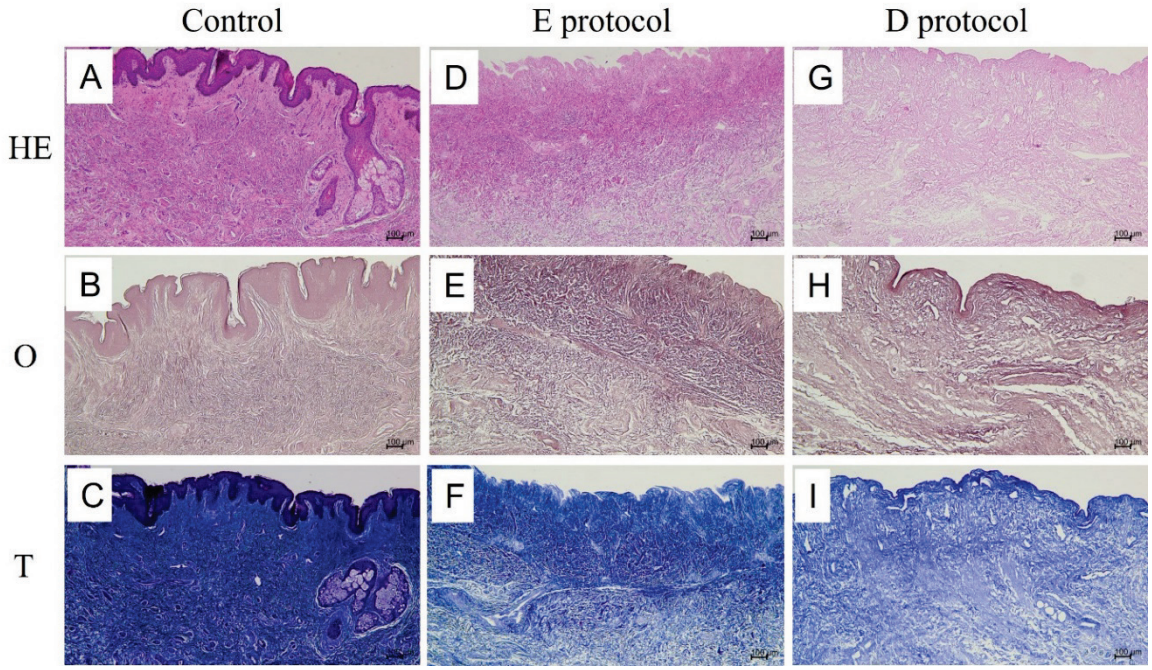

Fig. 3. Light microscopic comparison of native controls **(A-C)** vs. decellularized specimens **(D-I)**. **A-C** shows the normal morphology of the foreskin tissue stained with HE, orcein, and Masson´s trichrome, respectively. HE-stained foreskin control **(A)** shows the epithelial lining of the epidermis with a sebaceous gland and normally structured dermis with typical connective tissue components. The dermal layer contains elastic **(B)** and type I collagen fibers **(C)** crossing each other in different directions. Both the E protocol **(D,E,F)** and D protocol **(G,H,I)** of decellularization removed all cellular components, while at the same time preserving the structural integrity and density of elastic and collagen fibers of the ECM.

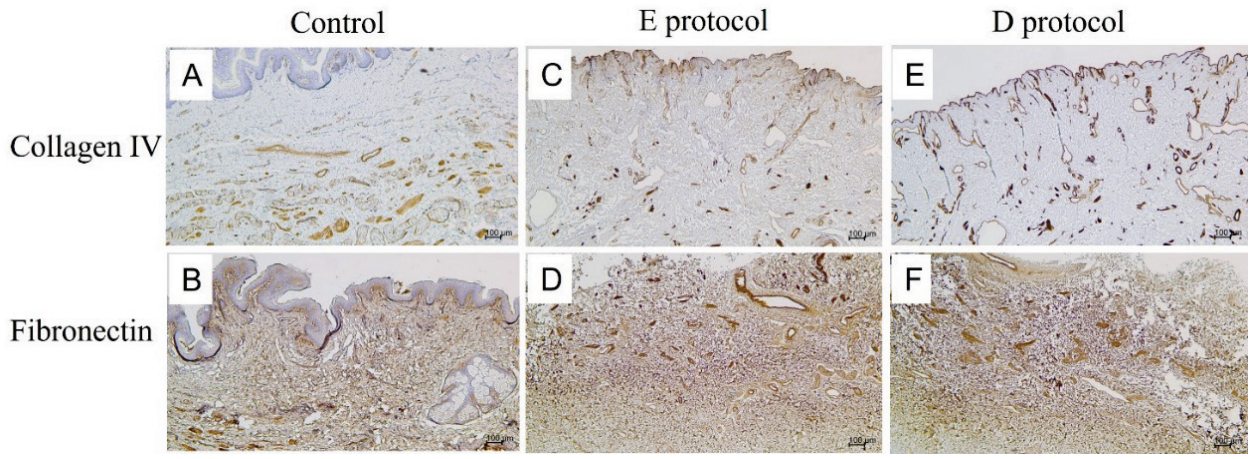

Fig. 4. Immunostaining for collagen IV and fibronectin in native controls **(A, B)** and decellularized specimens **(C-F)**. The native control stained for collagen IV **(A)** displays positivity mainly around blood vessels, and epithelial lining as the integral component of basal laminae. Both the E protocol **(C)** and D protocol **(E)** of decellularization preserved collagen IV as evidenced by the absence of any significant changes in collagen IV positivity after cell removal. Fibronectin in the native control **(B)** is widely distributed in the dermal layer as a crucial component of the ECM. In both the E protocol **(D)** and D protocol **(F)** of decellularization, fibronectin positivity is similar in distribution compared to native controls.

Preservation of histological morphology

Light microscopic examination of decellularized specimens revealed a complete absence of cell nuclei, indicating a thorough elimination of all cells and their components in both E and D protocols. The comparison between native HE-stained (Fig. 3A) and decellularized HE-stained specimens (Fig. 3D, 3G) demonstrates the success of the decellularization process. The preservation of ECM after decellularization was visualized using Masson's blue trichrome for type I collagen fibers (Fig 3F, 3I) and orcein for elastic fibers (Fig 3E, 3H). Compared to native controls, neither type I collagen fibers (Fig 3C) nor elastic fibers (Fig 3B) displayed any significant changes in density and structure to the extent which can be assessed at the light microscopic level. The fibers formed bundles that crossed each other in different directions.

After immunostaining for two other ECM components, namely type IV collagen (Fig. 4C, 4E) and fibronectin (Fig. 4D, 4F), their positivity was comparable to native controls (Fig 4A, 4B). All in all, at the light microscopic level, both the E (Fig. 4C, 4D) and D (Fig. 4E, 4F) decellularization protocols successfully removed all cellular components while at the same time preserving the structural integrity of the ECM.

SEM

Topography of the foreskin surface by the SEM confirmed an epithelial sloughing due to the decellularization process. Control samples (Fig. 5A, 5B) exhibited distinct epithelial layers of superficial stratified squamous keratinized epithelium. Epithelial cells were connected by cell junctions, which was obvious in the SEM micrograph (Fig. 5B) as well. The decellularization process resulted in epithelial desquamation, and the surface of the foreskin became naked and displayed the structural components of dermal lamina propria, mostly delicate collagen fibers in many directions (Fig. 5C). In the thick portion of the foreskin, dermal papillae (projections of lamina propria) were obvious, structural content of papilla was performed by collagen fibers (Fig. 5D).

DNA quantification and qualitative fragment analysis

The basic requirement for successful decellularization is the fulfillment of the criteria: the amount of DNA must not exceed 50 ng per mg of dry tissue weight, and the remaining DNA fragments must not be larger than 200 bp [23]. This is in addition to the absence of visible nuclei after HE or DAPI staining in decellularized tissue. Native foreskin samples contained a DNA concentration of 841.5 ± 61.5 ng/mg tissue, while decellularized samples contained a residual DNA content of 4.0 ± 5.6 ng/mg tissue for E protocol and 5.2 ± 7.3 ng/mg tissue for D protocol (Fig. 6A). Statistical analysis confirmed a significant difference in the amount of residual DNA ($p < 0.001$; $n = 12$). Qualitative analysis of DNA fragments by gel electrophoresis showed intact DNA bands in native foreskin samples larger than 3,000 base pairs (Fig. 6b). In the decellularized samples by both methods, the analysis confirmed significant removal of DNA.

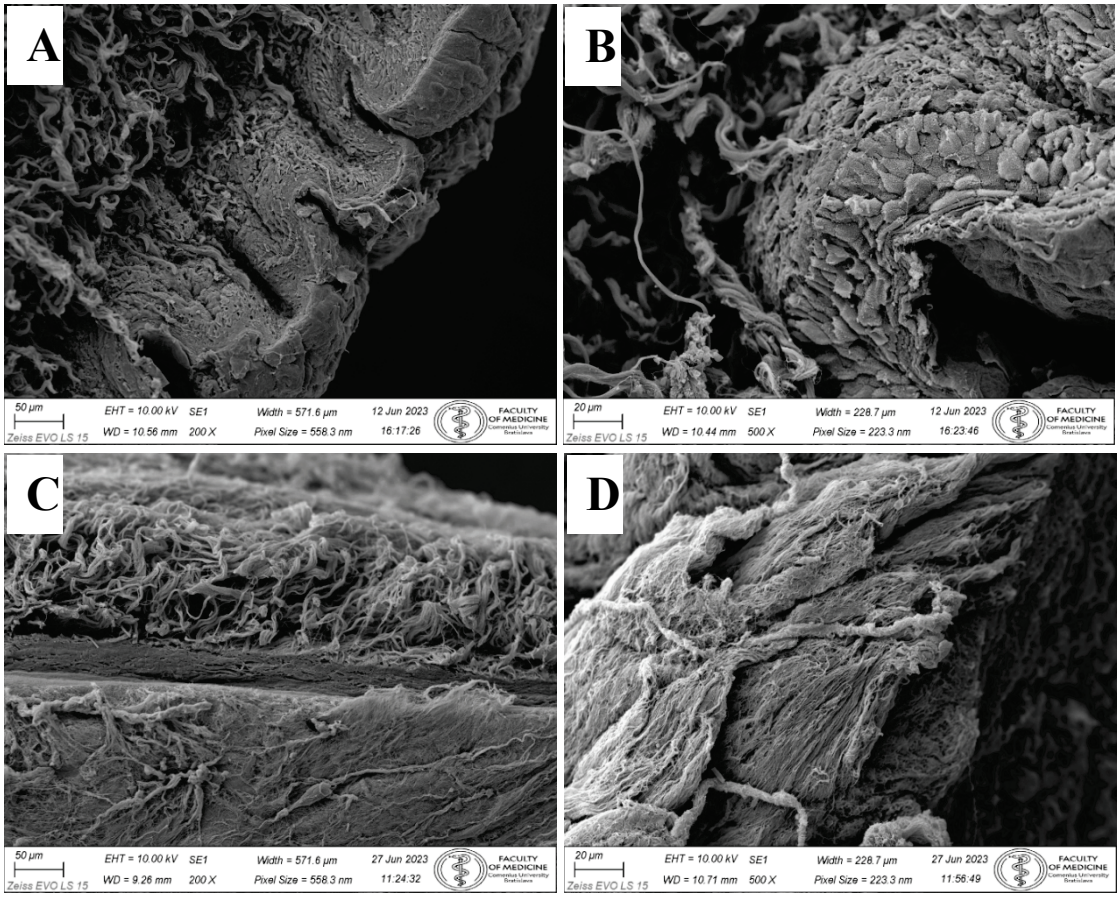

Fig. 5. Topography of control foreskin before the decellularization process by SEM. **A)** Stratified squamous keratinized epithelium covers the foreskin surface. Collagen fibers in underlying collagenous connective tissue form bundles in the dermis. Mag. 200x. **B)** Detail of all layers in the stratified squamous keratinized epithelium. Individual epithelial cells are closely packed and bound by intercellular connections. Mag. 500x. Topography of foreskin after the decellularization process by SEM. **C)** No epithelium is present on the sample surface. Only collagenous connective tissue of lamina propria remains. Collagen fibers in deep layers represent the foreskin reticular layer of the dermis. Mag. 200x. **D)** Naked surface of foreskin dermal papillae. Collagen fibers are evident. No epithelium is preserved. Mag. 500x.

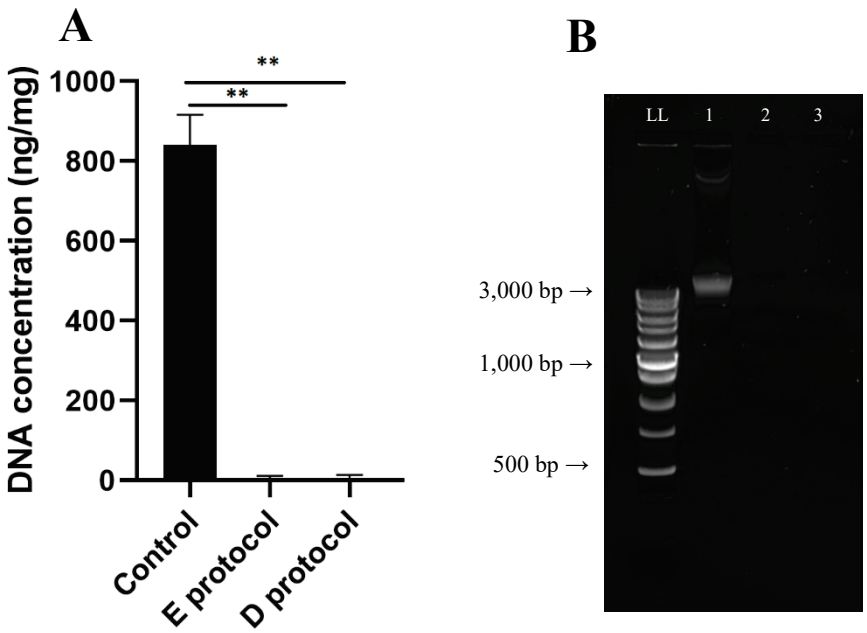

Fig. 6. A) Quantification of DNA in native and decellularized samples (ng/DNA per mg/tissue dry weight). Results as mean ± SD, n=6, **p≤0.001, t-test; **B)** Qualitative fragment length analysis of genomic DNA in 1.5 % agarose gel. LL length ladder, 1 - native foreskin sample, 2 - E protocol decellularized foreskin sample, 3 - D protocol decellularized foreskin sample.

Cytotoxicity

The MTT viability test results (Fig. 7) on the first, third, fifth, and seventh day show that ATSCs cells can proliferate in both control and matrix-conditioned medium. Data confirmed that the decellularized samples are not toxic and the matrix-conditioned medium did not contain soluble substances that would significantly impair cell viability. No confirmation of statistical significance was proven.

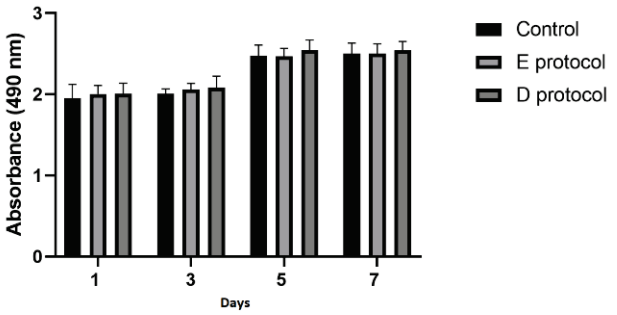

Fig. 7. Proliferation assessed by MTT test results. Test sample absorbance values on specific days. Data are presented as the mean ± SD. No significant decrease in the cell proliferation rate was detected when co-cultured with the matrix-conditioned medium.

Discussion

Research in regenerative medicine aims to create new forms of treatment as the gap between organ donors and recipients of transplants increases. Decellularization, in which the extracellular matrix is separated from its native cells and genetic material to create a natural scaffold, is one of the most promising methods for tissue and organ regeneration [23].

One of the most frequently utilized grafts in skin transplantation nowadays is an acellular dermal matrix. ADM can be produced from a variety of allogeneic or xenogeneic sources, including animal and human dermis. Strong clinical evidence already exists for the use of human ADM, but questions of access, cost, and ethics require consideration of a xenograft [24]. A solution to this dilemma could be to use the male foreskin as a source of tissue. Circumcision of the foreskin in males, either indicated for therapeutic purposes or planned for cultural or religious reasons, provides a rich supply of waste tissue that can be used as a skin graft without harming the donor. The prepuce is a pentalaminar structure composed of squamous mucosal epithelium, lamina propria, dartos muscle, dermis, and outer glabrous skin. The mucosa of the inner prepuce is lined by stratified squamous epithelium, similar to the frictional mucosa of the vagina, the inner eyelid, the mouth, or the esophagus [13].

ADM has already been used clinically in several genitourinary and reconstructive surgery cases. Chen and colleagues used autologous adipodermal graft and ADM for glans augmentation after penile prosthesis insertion [25]. In another case, an acellular matrix graft was incorporated during a procedure with an inadequate natural tissue bed to support an enduring surgical repair. In the particular case of hypospadias, the successful incorporation of an onlay graft of acellular matrix during the primary surgery may improve the quality of repair, leading to reduced complications [10]. Similarly, adipofascial flaps combined with ADM were used for the reconstruction of distal lower extremity defects. Losco *et al.* concluded that the use of such a combination is a reliable reconstructive option with low morbidity at the donor site and satisfactory results in terms of surgical and aesthetic outcomes [26]. It is evident that natural acellular tissue matrices present interesting novel biomaterials for reconstructive and regenerative surgery. Decellularized foreskin matrix, due to its size, could be ideal for use in the therapy of small dimensions.

In principle, decellularization can be achieved using chemical, enzymatic, physical, or combined processes, although each approach has advantages and disadvantages. The ECM can then be recellularized to create a functional tissue or organ, ideally retaining its natural structural, biochemical, and biomechanical characteristics [5]. Here we present two decellularization approaches enzymatic and detergent. Both of them led to the successful decellularization of the foreskin. Several decellularization protocols have been used previously, with maintaining the ECM components and the 3D structure of the foreskin ECM [27-29]. The majority of them applied SDS to remove cells with high efficacy, but SDS can solubilize nuclear and cytoplasmic membranes [23]. In D protocol we combined SDS with low-concentration ionic detergent Triton X100 and DNase I which led to cell and residual DNA removal without significant damage to ECM components. Utilization of the enzymatic approach led to similar results. In both techniques, all washing steps were done on an orbital shaker with mechanical agitation to increase the protocol's effectiveness. A similar dynamic mode of decellularization was applied by Simões and co-workers in the case of decellularization of the porcine urethra

[30]. Moreover, it was shown that combining mechanical and chemical decellularization methods is more efficient in cell and DNA removal and also supports maintaining the tissue architecture when compared with chemical decellularization [31].

We also evaluated potential cytotoxicity, because it is one of the most important prerequisites before clinical application of tissue-engineered substitutes. In both protocols, cytotoxicity testing did not display any inhibitory effect of the matrix-conditioned medium on cell viability compared to the control. The analysis of residual DNA also confirmed the effectiveness of both decellularization Techniques. After decellularization, we recorded a significant decrease in the amount of DNA present compared to the control below the limit set for tissue decellularization (50 ng per mg of dry tissue weight) [30]. This was also confirmed by the qualitative analysis of DNA fragments.

Overall, in this study, analyses performed so far have confirmed that both protocols represent a good starting point, but further research is needed before implementing these methods into routine practice. This in vivo and in vitro research will focus primarily on biosafety and biomechanical testing of decellularized ECM and the recellularization of these matrices.

Conclusion

The present study confirms the feasibility of foreskin decellularization based on enzymatic or detergent methods. Both techniques conserved the ultrastructure and composition of natural ECM while being DNA-free and non-toxic, making it an excellent scaffold for follow-up research and TE applications.

Conflict of Interest

There is no conflict of interest.

Acknowledgements

This publication was supported from the Operational Program Integrated Infrastructure for the project: Increasing the capacities and competences of the Comenius University in research, development, and innovation 313021BUZ3, co-financed from the resources of the European Regional Development Fund.

References

1. Neiva R, Giannobile WV. 16 - Mucosal and gingival tissue engineering. Joël Ferri, Ernst B. Hunziker (Editors). In: *Woodhead Publishing Series in Biomaterials, Preprosthetic and Maxillofacial Surgery, Woodhead Publishing*, 2011, Pp 305-326, ISBN 9781845695897. https://doi.org/10.1533/9780857092427.3.305
2. Mihalečko J, Boháč M, Danišovič Ľ, Koller J, Varga I, Kuniaková M. Acellular dermal matrix in plastic and reconstructive surgery. Physiol Res. 2022;71(Suppl 1):S51-S57. https://doi.org/10.33549/physiolres.935045
3. Ching C, Sett S, Walling S, Bezuhly M. Sternal cleft reconstruction with acellular dermal matrix and full-thickness calvarial graft. Eur J Cardiothorac Surg. 2023;63:ezad126. https://doi.org/10.1093/ejcts/ezad126
4. di Pompeo FS, Firmani G, Paolini G, Amorosi V, Briganti F, Sorotos M. Immediate prepectoral breast reconstruction using an ADM with smooth round implants: A prospective observational cohort study. J Plast Reconstr Aesthet Surg. 2023 May;80:56-65. https://doi.org/10.1016/j.bjps.2023.02.014
5. Lu W, Qi G, Ding Z, Li X, Qi W, He F. Clinical efficacy of acellular dermal matrix for plastic periodontal and implant surgery: a systematic review. Int J Oral Maxillofac Surg. 2020 Aug;49:1057-1066. https://doi.org/10.1016/j.ijom.2019.12.005
6. Yi CR, Jeon DN, Choi JW, Oh TS. Primary palatoplasty with intravelar veloplasty using acellular dermal matrix interpositional graft. J Craniofac Surg. 2021;32:252-256. https://doi.org/10.1097/SCS.0000000000006950
7. Chen B, Song H. Retrospective study of the application of acellular dermis in reconstructing full-thickness skin defects. Int Wound J. 2017;14:158-164. https://doi.org/10.1111/iwj.12576
8. Ayaz M, Najafi A, Karami MY. Thin split thickness skin grafting on human acellular dermal matrix scaffold for the treatment of deep burn wounds. Int J Organ Transplant Med. 2021;12:44-51.
9. Wang Y, Wang G, Hou X, Zhao Y, Chen B, Dai J, Sun N. Urethral tissue reconstruction using the acellular dermal matrix patch modified with collagen-binding vegf in beagle urethral injury models. Biomed Res Int. 2021;2021:5502740. https://doi.org/10.1155/2021/5502740

10. Morgante D, Radford A, Abbas SK, Ingham E, Subramaniam R, Southgate J. Augmentation of the insufficient tissue bed for surgical repair of hypospadias using acellular matrix grafts: A proof of concept study. J Tissue Eng. 2021 Apr 20;12:2041731421998840. https://doi.org/10.1177/2041731421998840
11. Tang X, Zhang X, Wu Y, Yin H, Du Y, Zhang X, Li Q, Liu S, Xu T. The clinical effects of utilizing allogeneic acellular dermal matrix in the surgical therapy of anterior urethral stricture. Urol Int. 2020;104:933-938. https://doi.org/10.1159/000510317
12. Zhang X, Chen X, Hong H, Hu R, Liu J, Liu C. Decellularized extracellular matrix scaffolds: Recent trends and emerging strategies in tissue engineering. Bioact Mater. 2021;10:15-31. https://doi.org/10.1016/j.bioactmat.2021.09.014
13. Fahmy, M.A.B. (2020). Histology of the Prepuce. In: Normal and Abnormal Prepuce. Springer, Cham. https://doi.org/10.1007/978-3-030-37621-5_6
14. Werker PM, Terng AS, Kon M. The prepuce free flap: dissection feasibility study and clinical application of a super-thin new flap. Plast Reconstr Surg. 1998;102:1075-1082. https://doi.org/10.1097/00006534-199809040-00024
15. Kigozi G, Wawer M, Ssettuba A, Kagaayi J, Nalugoda F, Watya S, Mangen FW, Kiwanuka N, Bacon MC, Lutalo T, Serwadda D, Gray RH. Foreskin surface area and HIV acquisition in Rakai, Uganda (size matters). AIDS. 2009;23:2209-13. https://doi.org/10.1097/QAD.0b013e328330eda8
16. Cox G, Morris BJ (2012). "Chapter 21: Why Circumcision:From Prehistory to the Twenty-First Century". In Bolnick DA, Koyle M, Yosha A (eds.). Surgical Guide to Circumcision. London: Springer-Verlag. pp. 243-259. ISBN 978-1-4471-2858-8. https://doi.org/10.1007/978-1-4471-2858-8_21
17. Siev M, Keheila M, Motamedinia P, Smith A. Indications for adult circumcision: a contemporary analysis. Can J Urol. 2016;23:8204-8208.
18. WHO. UNAIDS. WHO, UNAIDS press release on recommendations for male circumcision on prevention of HIV infection. March. 2007. https://www.unaids.org/en/resources/presscentre/pressreleaseandstatementarchive/2007/march/20070328whoandunaidsannouncerecommendationsfromexpe
19. Gray RH, Kigozi G, Serwadda D, Makumbi F, Watya S, Nalugoda F, Kiwanuka N, Moulton LH, Chaudhary MA, Chen MZ, Sewankambo NK, Wabwire-Mangen F, Bacon MC, Williams CF, Opendi P, Reynolds SJ, Laeyendecker O, Quinn TC, Wawer MJ. Male circumcision for HIV prevention in men in Rakai, Uganda: a randomised trial. Lancet. 2007;369:657-666. https://doi.org/10.1016/S0140-6736(07)60313-4
20. Bailey RC, Moses S, Parker CB, Agot K, Maclean I, Krieger JN, Williams CF, Campbell RT, Ndinya-Achola JO. Male circumcision for HIV prevention in young men in Kisumu, Kenya: a randomised controlled trial. Lancet 2007;369:643-656. https://doi.org/10.1016/S0140-6736(07)60312-2
21. Fang F, Ni K, Cai Y, Ye Z, Shang J, Shen S, Xiong C. Biological characters of human dermal fibroblasts derived from foreskin of male infertile patients. Tissue Cell 2017;49:56-63. https://doi.org/10.1016/j.tice.2016.12.003
22. Werker PM, Terng AS, Kon M. The prepuce free flap: dissection feasibility study and clinical application of a super-thin new flap. Plast Reconstr Surg 1998;102:1075-1082. https://doi.org/10.1097/00006534-199809040-00024
23. Gilpin A, Yang Y. Decellularization strategies for regenerative medicine: from processing techniques to applications. Biomed Res Int. 2017;2017:9831534. https://doi.org/10.1155/2017/9831534
24. Saricilar EC, Huang S. Comparison of porcine and human acellular dermal matrix outcomes in wound healing: a deep dive into the evidence. Arch Plast Surg. 2021;48:433-439. https://doi.org/10.5999/aps.2020.02306
25. Chen ML, Sun HH, Kasabwala K, Freniere B, Moses RA. Glans adipodermal augmentation for management of neophallus fat atrophy after penile implant insertion: Surgical technique and outcomes. Urology. 2023:S0090-4295(23)00468-5. https://doi.org/10.1016/j.urology.2023.05.023
26. Losco L, Sereni S, Aksoyler D, Spadoni D, Bolletta A, Cigna E. Perforator-based Adipofascial Flaps and ADM: A Novel Combined Approach to Distal Lower Extremity Defects. Plast Reconstr Surg Glob Open 2022;10:e4131. https://doi.org/10.1097/GOX.0000000000004131

27. Purpura V, Bondioli E, Cunningham EJ, De Luca G, Capirossi D, Nigrisoli E, Drozd T, Serody M, Aiello V, Melandri D. The development of a decellularized extracellular matrix-based biomaterial scaffold derived from human foreskin for the purpose of foreskin reconstruction in circumcised males. J Tissue Eng 2018;9:2041731418812613. https://doi.org/10.1177/2041731418812613
28. Cui H, Chai Y, Yu Y. Progress in developing decellularized bioscaffolds for enhancing skin construction. J Biomed Mater Res A 2019;107:1849-1859. https://doi.org/10.1002/jbm.a.36688
29. Rahmati S, Jalili A, Dehkordi MB, Przedborski M. An effective method for decellularization of human foreskin: implications for skin regeneration in small wounds. Cell J 2022;24:506-514.
30. Simões IN, Vale P, Soker S, Atala A, Keller D, Noiva R, Carvalho S, Peleteiro C, Cabral JM, Eberli D, da Silva CL, Baptista PM. Acellular urethra bioscaffold: decellularization of whole urethras for tissue engineering applications. Sci Rep 2017;7:41934. https://doi.org/10.1038/srep41934
31. Consolo F, Brizzola S, Tremolada G, Grieco V, Riva F, Acocella F, Fiore GB, Soncini M. A dynamic distention protocol for whole-organ bladder decellularization: histological and biomechanical characterization of the acellular matrix. J Tissue Eng Regen Med 2016;10:E101-112. https://doi.org/10.1002/term.1767